

*Supplementary Information for*

**Photoinduced Luminescence Activation of Hydrophilic ‘Caged’ Carbons Dots**

*Aviya S. Akari Maria R. Narciso, Emmanuel O. Fagbohun, Pedro D. Ortiz,  
Roberto J. Botelho and Stefania Impellizzeri\**

Department of Chemistry and Biology, Toronto Metropolitan University, 350 Victoria St., Toronto, ON, M5B 2K3, Canada

**Content**

<b>Materials and methods</b>	<b>S2</b>
<b>Synthesis of N-doped, COOH functionalized carbon dots (CDs 1)</b>	<b>S3</b>
<b>Conjugation of 2-Nitrobenzylamine to CDs (synthesis of 2NB-CDs 2)</b>	<b>S3</b>
<b>Synthesis of model quencher compound 2NB-OMe (3)</b>	<b>S4</b>
<b>Cell culture and pinocytosis of CDs 1</b>	<b>S4</b>
<b>Cell culture and photoinduced uncaging of 2NB-CDs 2</b>	<b>S5</b>
<b>Live-cell confocal microscopy</b>	<b>S5</b>
<b>Image and statistical analysis</b>	<b>S5</b>
<b>Figure S1. TEM images and size distribution of CDs 1</b>	<b>S6</b>
<b>Figure S2. DLS profile and zeta potential of CDs 1</b>	<b>S7</b>
<b>Figure S3. XPS spectrum of CDs 1</b>	<b>S8</b>
<b>Figure S4. High-resolution XPS spectra for C, O, N and Cl of CDs 1</b>	<b>S9</b>
<b>Figure S5. FT-IR spectrum of CDs 1</b>	<b>S10</b>
<b>Figure S6. <sup>1</sup>H NMR spectrum of CDs 1 in D<sub>2</sub>O</b>	<b>S11</b>
<b>Figure S7. <sup>13</sup>C NMR spectrum of CDs 1 in D<sub>2</sub>O</b>	<b>S11</b>
<b>Figure S8. <sup>1</sup>H NMR spectrum of glucosamine hydrochloride and β-alanine in D<sub>2</sub>O</b>	<b>S12</b>
<b>Figure S9. <sup>1</sup>H NMR spectrum of CDs 1 in CDCl<sub>3</sub></b>	<b>S12</b>
<b>Figure S10. Spectroscopic data for determining the quantum yield of CDs 1</b>	<b>S13</b>
<b>Figure S11. Emission spectrum of glucosamine hydrochloride and β-alanine</b>	<b>S14</b>
<b>Figure S12. Emission quenching and Stern-Volmer plot of CDs 1 with increasing amounts of 3</b>	<b>S15</b>
<b>Voltammetry of CDs (Fig. S13 and discussion)</b>	<b>S16</b>
<b>Figure S14. Emission spectra of CDs 1 before and after UVA irradiation (photostability)</b>	<b>S17</b>
<b>Figure S15. Emission of 2NB-CDs 2 before and after UVA in H<sub>2</sub>O pH 3 and 50:50 H<sub>2</sub>O:DMSO</b>	<b>S18</b>
<b>Figure S16. Microscopy and statistical analysis of RAW 264.7 exposed to 2NB-CDs 2</b>	<b>S19</b>

## Materials and methods

All reagents were purchased from Sigma Aldrich and Fisher Scientific. Solvents were purchased from ACP. The use of organic solvents in this study was conducted within a fume hood to ensure proper containment and ventilation. Ultrapure deionized water (MilliQ, 18.2 MΩ) was obtained from a Millipore Purification System. Reactions were monitored by thin-layer chromatography using aluminum-backed sheets coated with 200 μm silica (60, F<sub>254</sub>). SiliaFlash® P60, 40-63 mm (230-400 mesh) silica gel from SiliCycle was used for the purification of compound **3** by column chromatography. NMR spectra were recorded at room temperature with a Bruker Avance 400 spectrometer. Steady-state absorption spectra were recorded with an Agilent Cary 60 UV-visible spectrometer using quartz cells with a path length of 1 cm. Steady-state emission spectra were recorded with an Agilent Cary Eclipse spectrometer using quartz cells. Slit widths were chosen as 10:10, and detector voltage was set at 600 V. Illumination at 365 nm was performed with a Luzchem LCZ-4 photoreactor equipped with 8 UVA bulbs (8 W each). XPS spectra were acquired with a K-Alpha XPS system (ThermoFisher Scientific, East Grinstead, UK) at the Ontario Centre for the Characterization of Advanced Materials (OCCAM). The X-ray source was monochromatized Al K-Alpha, 400 μm spot size (2:1 ellipse, with the major axis being the noted spot size). Data was acquired at a nominal take-off angle of 90°. Survey spectra were acquired at a pass energy of 200 eV. The corresponding point density on the energy axis was 1eV/step. Regional scans were performed at high energy resolution (lower pass energy 50 eV), and with correspondingly higher point density on the energy axis, 0.1 eV between points. The dwell time for the acquisition of these spectra was 50 ms. XPS data was processed using Thermo Scientific Avantage software. Surface elemental compositions were calculated from background-subtracted (smart background) peak areas derived from transmission function-corrected regional spectra. Sensitivity factors used to calculate the relative atomic percentages were provided by the instrument manufacturer. FT-IR Diamond ATR spectra were recorded with a Cary 630 spectrometer by Agilent Technologies. Samples for electron microscopy were prepared by drop-casting a dilute solution of CDs onto carbon square mesh copper TEM grids (Electron Microscopy Sciences) before drying overnight under ambient conditions in the fume hood. TEM images were recorded with a Hitachi S-5200 operating at 5.0 kV acceleration voltage. Freeze drying was performed using a Labconco FreeZone 2.5 attached to a vacuum pump (Edwards 117 RV5). The temperature for the freeze dryer was set at -50 °C. Dynamic Light Scattering (DLS) and zeta

potential measurements were carried out using a Zetasizer Advance Series Ultra (Malvern Instruments). Measurements were performed at 25 °C using a 633 nm He–Ne laser and a backscattering angle of 173°. The medium had a refractive index of 1.330 and a viscosity of 0.8872 mPa·s, while the material refractive index was set to 0.200. Prior to analysis, samples were filtered through a 0.22 µm PTFE membrane. Each sample was measured in triplicate, and the reported values represent the averaged results. Electrochemical measurements were performed with a Metrohm Autolab Type II potentiostat/galvanostat. CV were run under N<sub>2</sub> in dimethylformamide (DMF) using 0.1 M Bu<sub>4</sub>NPF<sub>6</sub> as supporting electrolyte, 1 mg/mL of dialyzed CDs, a glassy-carbon working electrode (3 mm), a platinum counter electrode, and an Ag/AgCl (KCl 3M) reference. The scan rate was set at 0.1 V s<sup>-1</sup>. The use of ferrocene as an internal standard was prevented by the fact that its oxidation process becomes irreversible in the presence of the carbon dots. However, the potential of the aqueous Ag/AgCl reference electrode remained stable under our operating conditions.

### **Synthesis of N-doped, COOH (surface) functionalized carbon dots (CDs 1)**

CDs were synthesized based on an adapted literature procedure.<sup>1</sup> Glucosamine hydrochloride (1 g, 4.63 mmol) was dissolved in MilliΩ H<sub>2</sub>O (20 mL) in a 250 mL Erlenmeyer flask. β-alanine (0.45 g, 5.09 mmol) was added to the solution and stirred until dissolved. The stirring bar was removed, and the flask was placed in a domestic microwave, where the solution was heated at maximum power for 2 minutes. A viscous brown residue was obtained, which was then dissolved in H<sub>2</sub>O (20 mL) and centrifuged twice (8500 rpm, 30 mins). The supernatant was collected and concentrated via lyophilization (freeze drying) to yield the carbon dots as a brown viscous product. FT-IR ATR (Figure S5): 3320 cm<sup>-1</sup> (ν<sub>s</sub>, O–H and N–H); 2900 cm<sup>-1</sup> (ν<sub>s</sub>, C–H sp<sup>3</sup>); 1714 cm<sup>-1</sup> (ν<sub>s</sub>, C=O); 1599 cm<sup>-1</sup> (ν<sub>b</sub>, N–H); 1405 cm<sup>-1</sup> (ν<sub>s</sub>, C–N); 1196 cm<sup>-1</sup> (ν<sub>s</sub>, C–N or C–O); 805 cm<sup>-1</sup> (ν<sub>b</sub>, N–H, oop).

### **Conjugation of 2-Nitrobenzylamine to CDs 1 (synthesis of 2NB-CDs 2)**

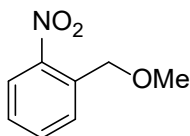
CDI (1,1-carbonyldiimidazole, 40 mg) was added to a solution of CDs 1 (10 mg) in distilled H<sub>2</sub>O (1 mL). The solution was sonicated for 15 min, after which 2-nitrobenzylamine hydrochloride (2

---

<sup>1</sup> S. A. Hill, D. Benito-Alifonso, S. A. Davis, D. J. Morgan, M. Berry and M. C. Galan, *Sci. Rep.*, 2018, **8**, 12234.

mL of a 2.75 mg/mL aqueous solution) was added, and the mixture was stirred for 24 h in the dark. The modified particles were then dialyzed against MilliQ H<sub>2</sub>O for 2 days using dialysis membrane tubing with (100-500 Da). The dialyzed solution was lyophilized (freeze-dried) to yield brown particles (~8.5 mg).

### Synthesis of model quencher compound 2NB-OMe (3)



**2NB-OMe (3)**

2-nitrobenzyl alcohol (1 g, 0.653 mmol) was dissolved in a mixture of 50% aqueous NaOH (1.36 g, 0.17 mmol) and petroleum ether (5 mL). Using an addition funnel, benzyl triethylammonium chloride (20 mg) was added to the mixture, followed by dimethyl sulfate (1.064 g, 8.4 mmol). The mixture was stirred until homogeneous, after which 0.1 mL of dimethyl sulfate was added, and the reaction was stirred for 1 hour. Ammonium formate (1.28 g) was then added to quench the excess dimethyl sulfate. The crude was transferred to a separatory funnel. The organic phase was collected, and the aqueous phase was washed with an additional 5 mL of petroleum ether. The organic fractions were combined and concentrated under reduced pressure, yielding **3** (1.044 g, 95.6 %) as a light orange oil. <sup>1</sup>H NMR (400 MHz, CDCl<sub>3</sub>): δ 8.07-8.05 (1H, d), 7.78-7.76 (1H, d), 7.66-7.62 (1H, t), 7.45- 7.41 (1H, t), 4.83 (2H, s), 3.48 (3H, s). <sup>13</sup>C {<sup>1</sup>H} NMR (100 MHz, CDCl<sub>3</sub>): δ 135.10, 133.65, 128.52, 127.91, 124.65, 71.11, 58.91.

### Cell culture and pinocytosis of CDs 1

The RAW 264.7 macrophage-like cell line originated from a male mouse (TIB-71, ATCC, Manassas, VA) and was maintained in Dulbecco's Modified Eagle Medium (DMEM) supplemented with 10% heat-inactivated fetal bovine serum (FBS) and 1% penicillin-streptomycin at 37°C and 5% CO<sub>2</sub>. For each experiment, RAW 264.7 macrophages were seeded on 18-mm coverslips overnight in complete DMEM medium. To allow pinocytic uptake of the carbon dots,

cells were pulsed with 30 mg/ml CDs **1** for 30 minutes, washed 3 times with 1X PBS, and chased for 30 minutes in fresh medium at 37°C and 5% CO<sub>2</sub> before imaging.

### **Cell culture and photoinduced uncaging of 2NB-CDs **2****

RAW 264.7 macrophages were seeded and grown as above but pulsed with 50 mg/ml 2NB-CDs **2** for 10-30 minutes, washed 3 times with 1X PBS, and chased for 30 minutes simultaneous with ultraviolet illumination. Incubation was performed at 37°C and 5% CO<sub>2</sub>. Alternatively, 2NB-CDs **2** were pre-exposed to UVA light before pinocytosis.

### **Live-cell confocal microscopy**

Live cell imaging was done using a Quorum Diskovery spinning disc confocal microscope equipped with a Leica DMI8 connected to an iXON EMCCD camera controlled by the MetaMorph software using a 63X oil objective. 405 nm, 488 nm, and 561 nm lasers were used to excite the CDs. To detect fluorescence, 450 nm/55 nm, 525 nm/50 nm, and 600 nm/50 nm emission filters listed with their corresponding bandwidth were used. During live-cell microscopy, cells were maintained in phenol-free DMEM supplemented with 10% fetal bovine serum and 1% penicillin-streptomycin within an environment chamber set to 37°C and 5% CO<sub>2</sub>. Images were acquired using a single z-plane.

### **Image and statistical analysis**

Image processing was done with ImageJ/FIJI. Each cell was selected as a region of interest and its mean fluorescence intensity was quantified, followed by background correction. Graphs are presented as superplots to display individual data points (cells) and averages for three independent trials represented as large, outlined symbols. Data are shown as mean ± Standard Error of the Mean. GraphPad Prism 10 was used to generate graphs and statistically analyze data using a paired, one-tailed Student's t-test. Significant comparisons are displayed as p-values, using a threshold of p<0.05 for statistically significant differences.

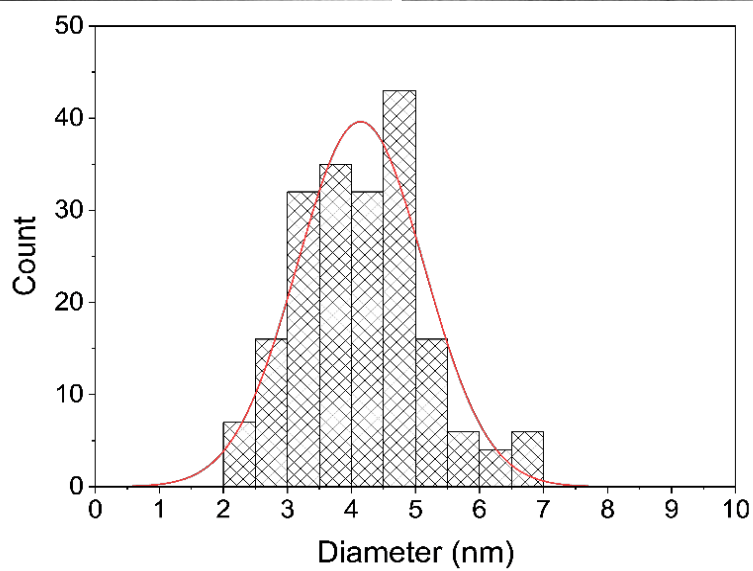
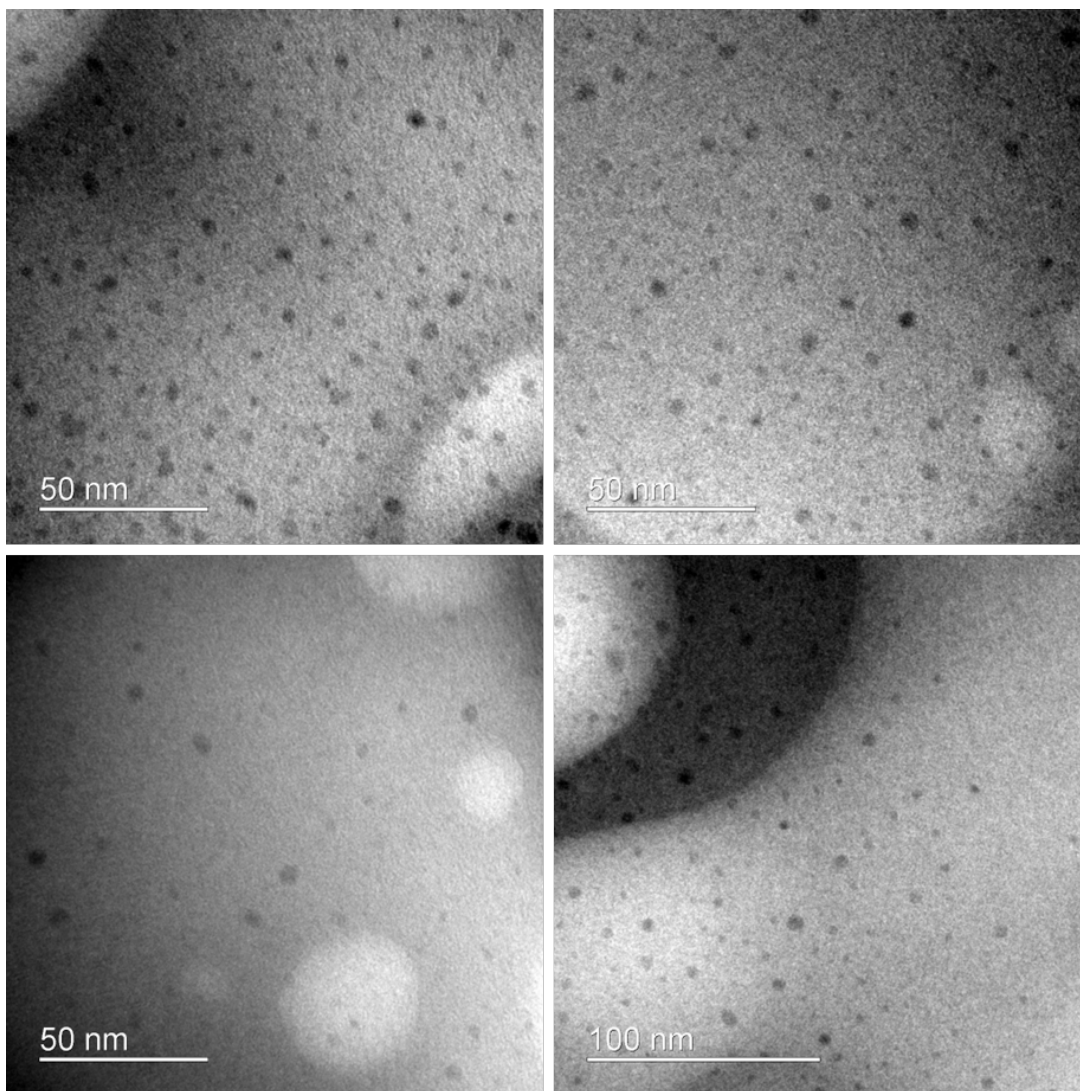


**Figure S1.** Representative transmission electron microscopy images and size distribution of CDs 1.

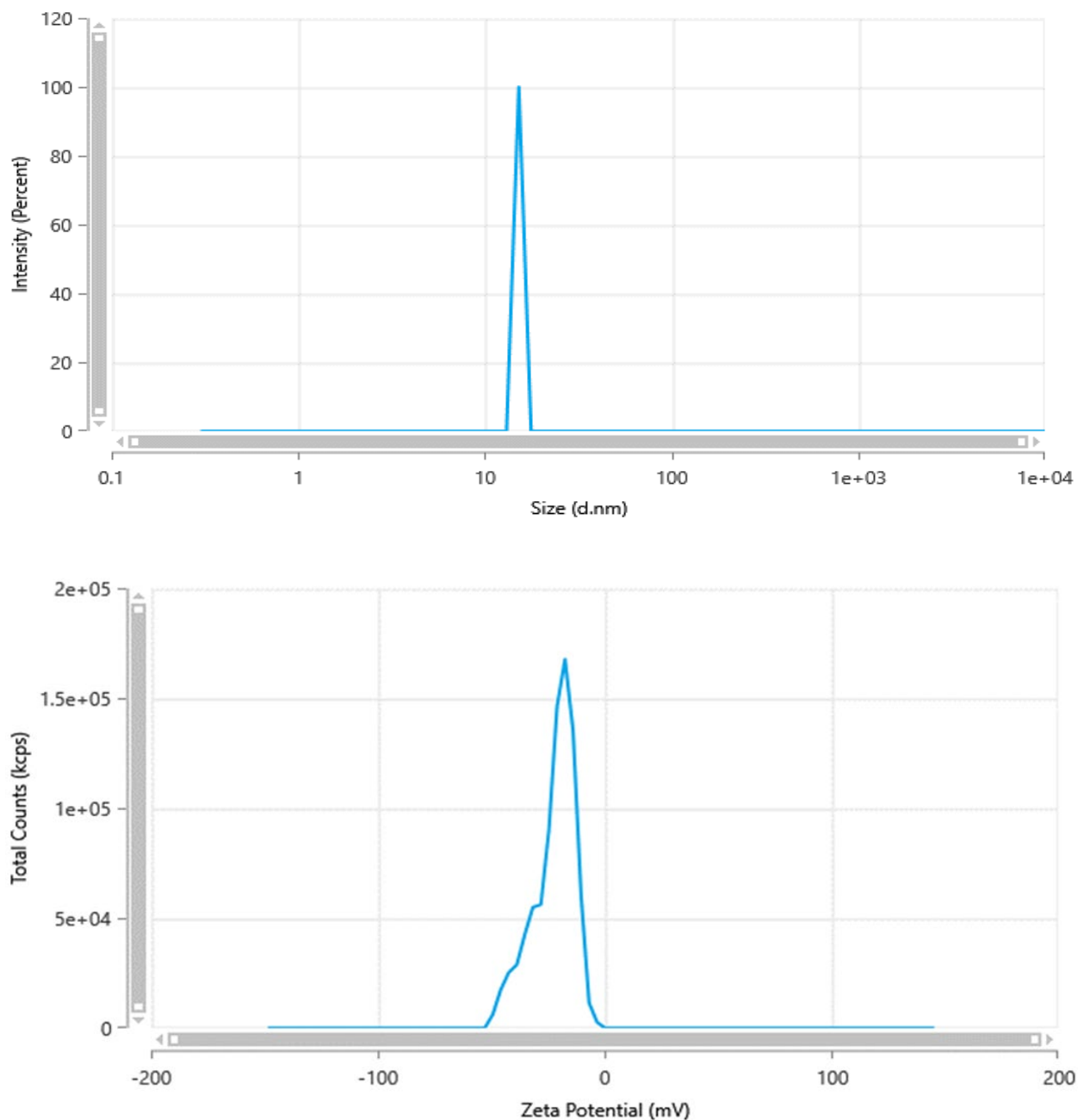


**Figure S2.** DLS profile and zeta potential of CDs 1. The aqueous dispersion of CDs was filtered through a 0.22  $\mu\text{m}$  PTFE membrane to remove large or aggregated particles. The resulting filtrate was subsequently purified by size-exclusion chromatography using Sephadex G-25 gel (Sigma-Aldrich) as the stationary phase and MilliQ water as the eluent. The standard deviation for the zeta potential is 4.14. We note that the polydispersity index (PDI), as determined by DLS, was consistently reported as 1, which may be indicative of measurement limitations or instrumental artifacts rather than true sample heterogeneity.

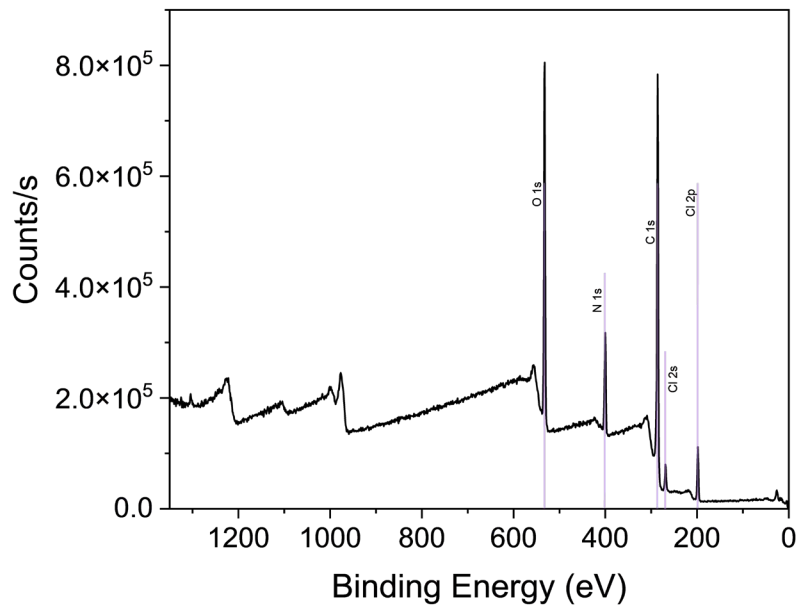


**Figure S3.** XPS spectrum of CDs 1.

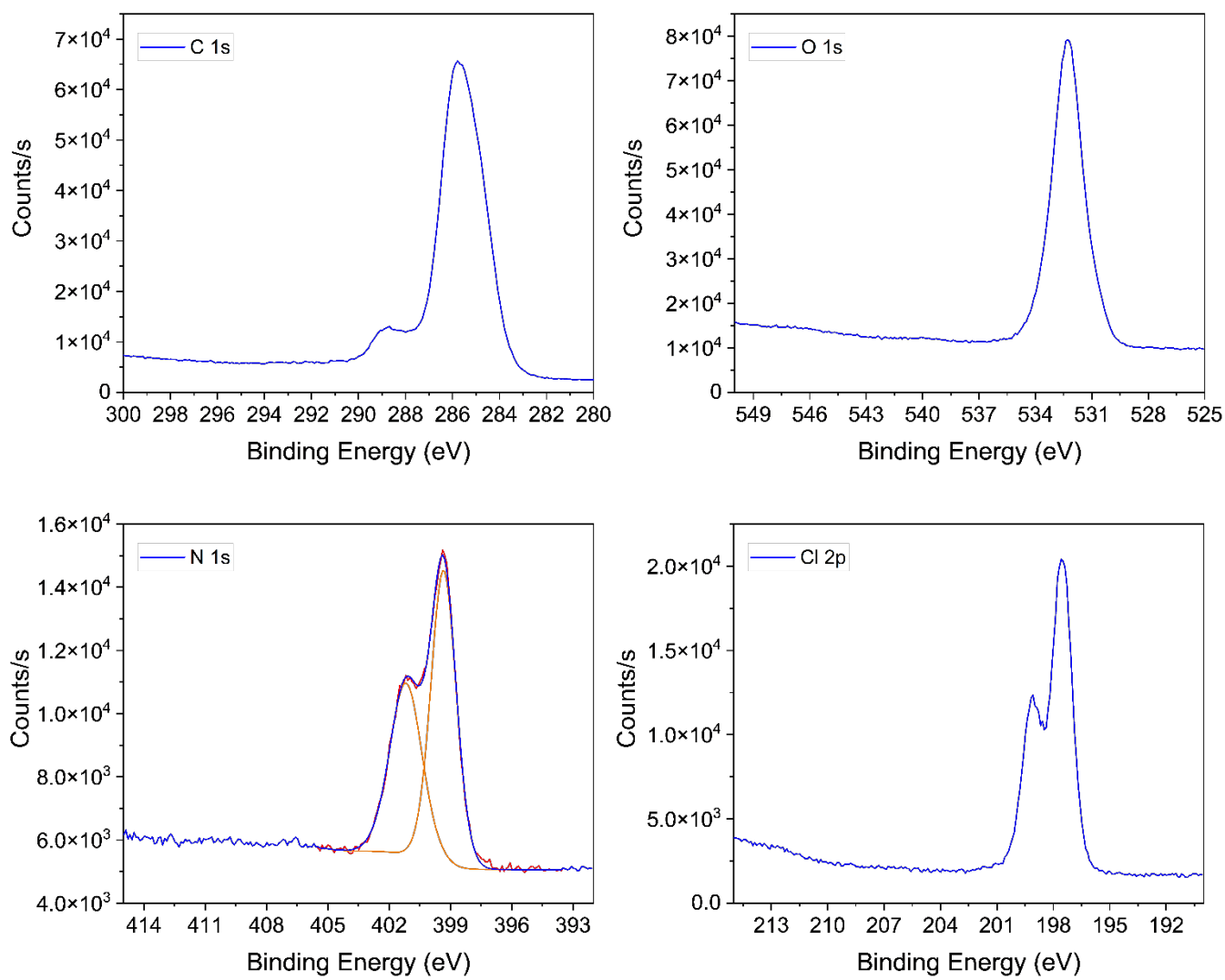


**Figure S4.** High-resolution XPS spectra for C, O, N and Cl of CDs 1.

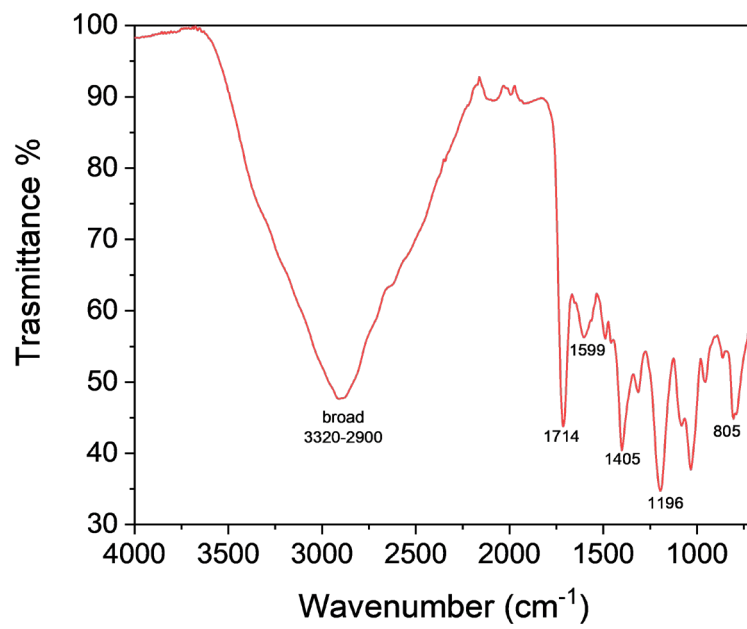


**Figure S5.** FT-IR spectrum of CDs 1.

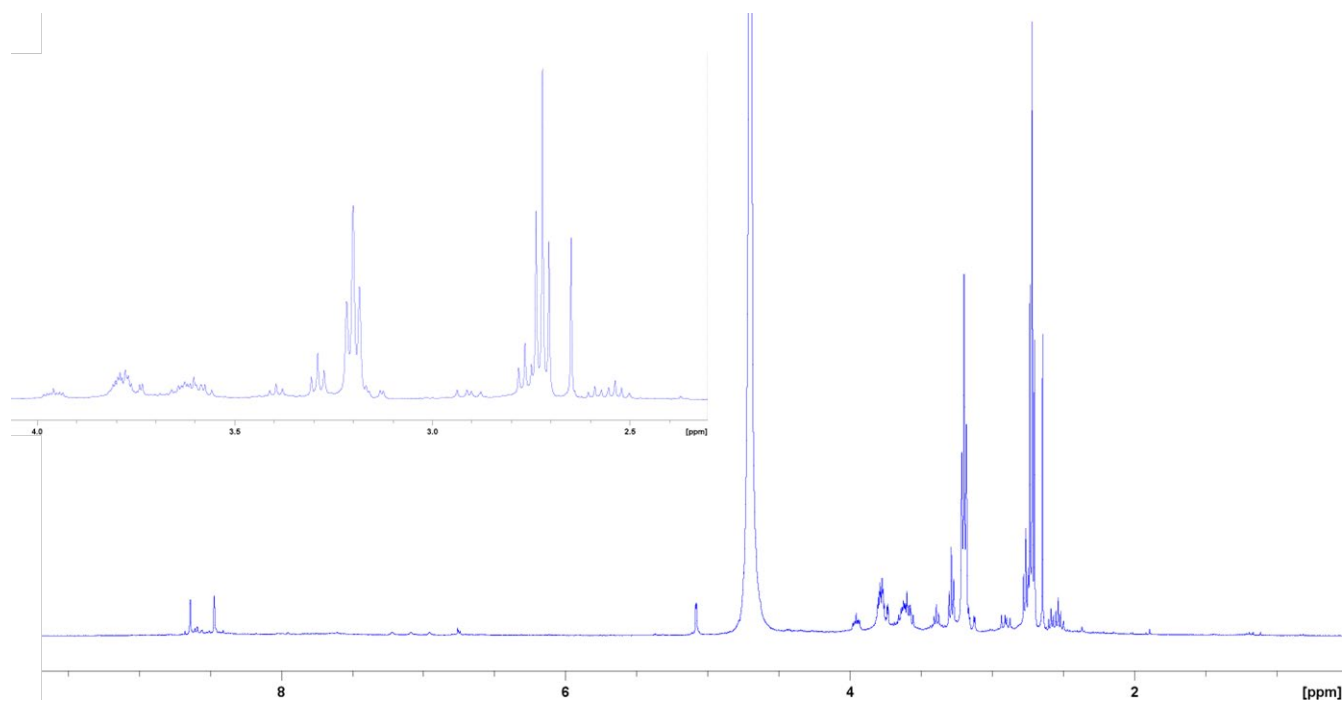


**Figure S6.**  $^1\text{H}$  NMR spectrum ( $\text{D}_2\text{O}$ , 20 °C, 400 MHz) of CDs **1**.

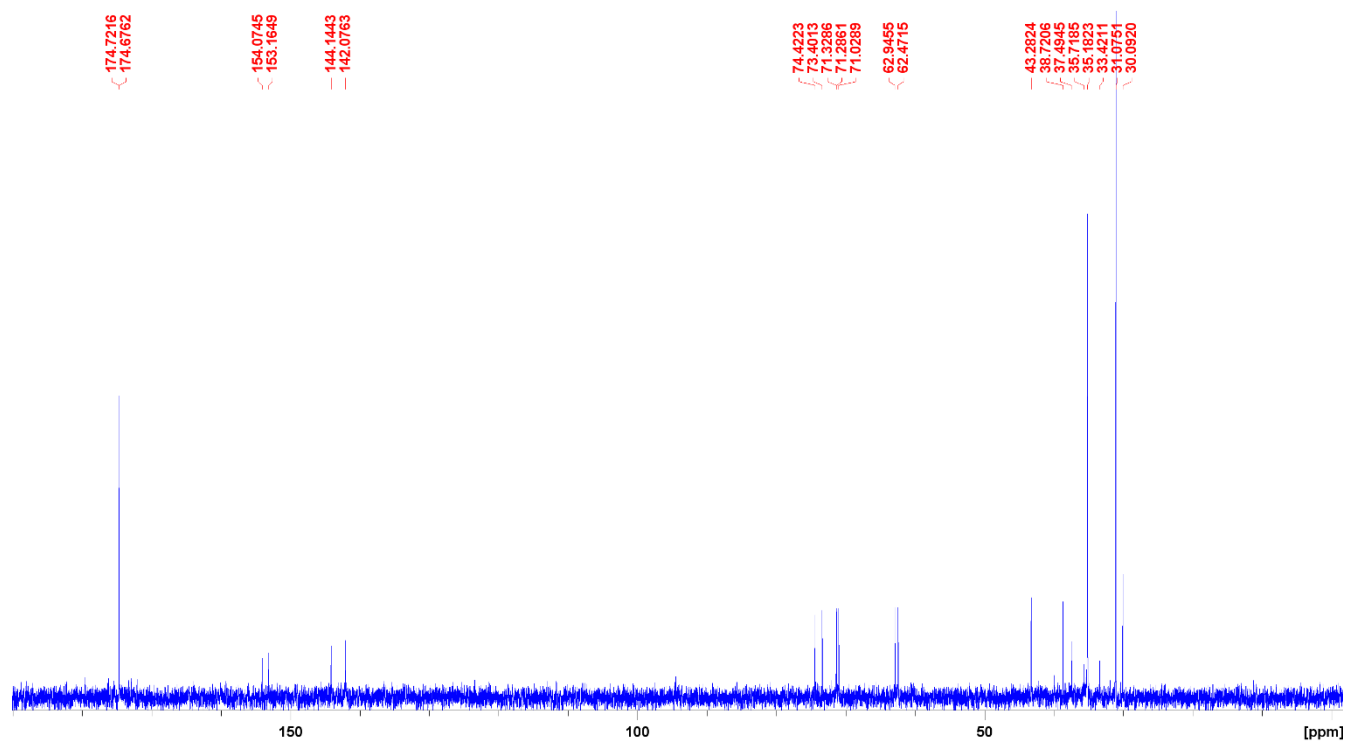


**Figure S7.**  $^{13}\text{C}$  NMR spectrum ( $\text{D}_2\text{O}$ , 20 °C, 100 MHz) of CDs **1**.

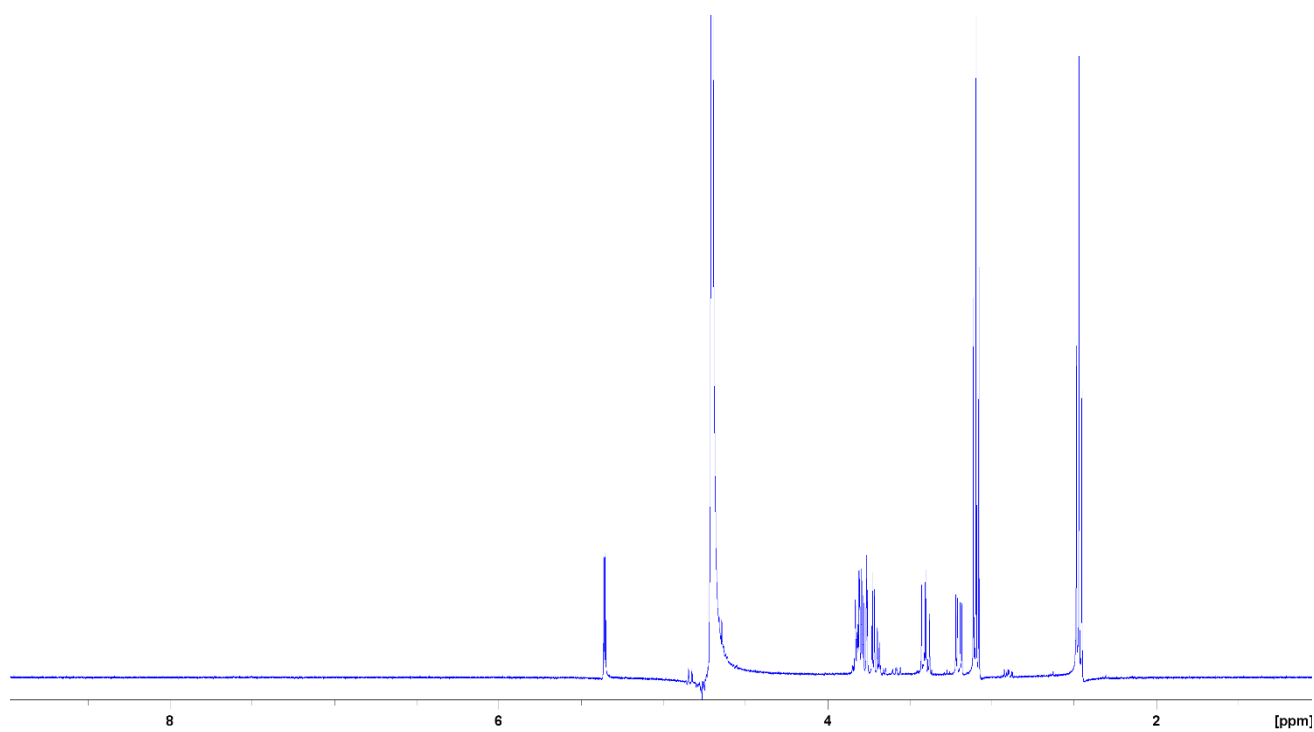


**Figure S8.** <sup>1</sup>H NMR spectrum (D<sub>2</sub>O, 20 °C, 400 MHz) of a mixture of glucosamine hydrochloride and β-alanine before MW treatment.

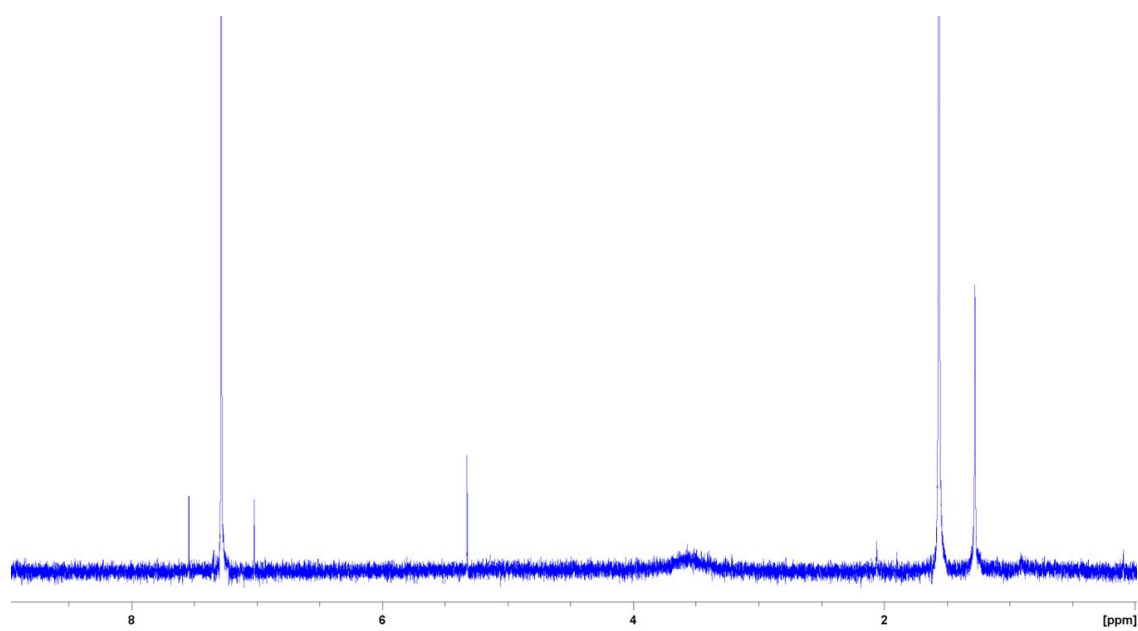


**Figure S9.** <sup>1</sup>H NMR spectrum (CDCl<sub>3</sub>, 20 °C, 400 MHz) of CDs **1**.

The quantum yield ( $\Phi$ ) of luminescence of CDs **1** was calculated using the optically diluted method and 4',6-diamidino-2-phenylindole (DAPI,  $\Phi = 0.04$  in its free [unbound] form)<sup>2</sup> as reference (denoted by subscript *R* below). The excitation wavelength was 340 nm, and emission spectra were integrated from 360 to 650 nm. The quantum yield of fluorescence was then computed according to the following equation:

$$\Phi = \Phi_R \frac{I}{I_R} \frac{A_R}{A} \left( \frac{\eta}{\eta_R} \right)^2$$

where *I*, *A* and  $\eta$  represent integrated fluorescence intensity, absorption (below 0.1) at the excitation wavelength, and refractive index of the solvent (water), respectively. The calculated  $\Phi$  of CDs **1** (average of 8 measurements, Figure S10) is 0.08 (8%).

A@340 nm (CDs <b>1</b> )	A <sub>R</sub> @340 nm (DAPI)	I (CDs <b>1</b> )	I <sub>R</sub> (DAPI)	$\Phi$ (CDs <b>1</b> )
0.02006	0.02047	15988	9298	0.07
0.03081	0.03006	23679	12896	0.072
0.04967	0.03984	36790	16257	0.092
0.06072	0.05055	46263	21155	0.087
0.07245	0.0601	53379	24555	0.085
0.07966	0.07097	59658	28834	0.083
0.09047	0.08035	65793	32589	0.08
0.10774	0.09004	73301	40117	0.068

**Figure S10.** Spectroscopic data for determining the quantum yield of CDs **1**.

<sup>2</sup> T. Härd, P. Fan, D. R. Kearns *Photochem. Photobiol.* 1990, **51**, 77; P. Cavatorta, L. Masotti, A. G. Szabo, *Biophys. Chem.* 1985, **22**, 11; Estandarte, S. Botchway, C. Lynch et al. *Sci Rep* 2016, **6**, 31417.

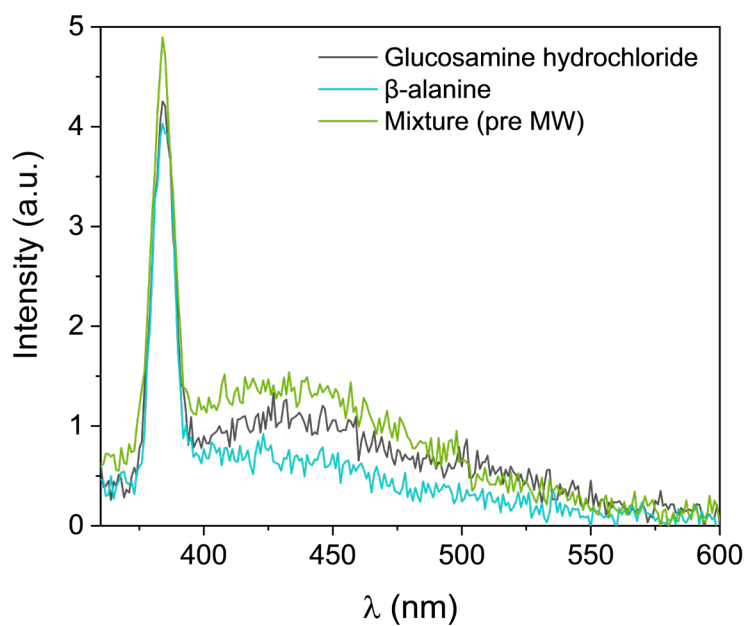


**Figure S11.** Emission spectrum (1 mg/ml,  $\lambda_{\text{Ex}} = 340$  nm, 20 °C, H<sub>2</sub>O) of a mixture of glucosamine hydrochloride and  $\beta$ -alanine before MW treatment. The mass ratio in the mixture is identical to that used for the synthesis of CDs **1**.

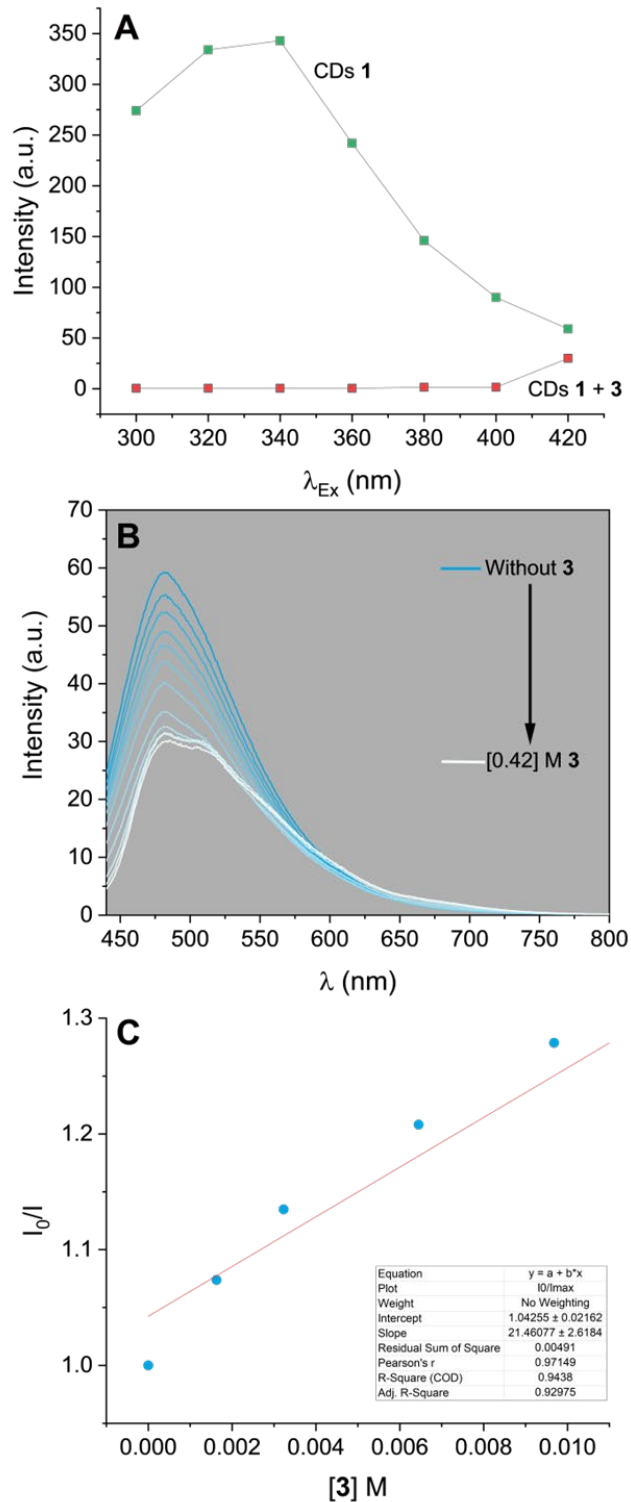


**Figure S12.** Emission intensity (A, 10  $\mu\text{g/mL}$ , 20  $^\circ\text{C}$ ,  $\text{CH}_3\text{OH}$ ) of CDs **1** before and after addition of **3** [0.42 M] under different excitation conditions. Emission spectra at  $\lambda_{EX} = 420$  nm (B, 10  $\mu\text{g/mL}$ , 20  $^\circ\text{C}$ ,  $\text{CH}_3\text{OH}$ ) of CDs **1** before and after the addition of increasing amounts of **3**. Dependence of the emission intensity (C) of CDs **1** measured at  $\lambda_{EX} = 420$  nm on the concentration of **3**. The red line in C represents the linear fitting of the represented data.

## Voltammetry of CDs 1 (Fig. S13) and discussion

The free energy change ( $\Delta G^\circ$ ) for the photoinduced electron transfer process was estimated with the Rehm-Weller equation:

$$\Delta G^\circ = eE_{Ox} - eE_{Red} - \Delta E_{00} + \frac{e^2}{4\pi\epsilon_0\epsilon_r d}$$

where  $e$  is the elementary charge,  $E_{Ox}$  is the oxidation potential of the species donating the electron,  $E_{Red}$  is the reduction potential of the species accepting the electron,  $\Delta E_{00}$  is the optical band gap of the carbon dots,  $\epsilon_0$  is the vacuum permittivity,  $\epsilon_r$  is the dielectric constant of the medium, and  $d$  is the distance between donor and acceptor.<sup>3</sup> The inclusion of  $\Delta E_{00}$  makes it clear that this equation can only be used to model *photoinduced* electron transfer. The redox potentials of the carbon nanoparticles are +1.43 V vs Ag/AgCl (average of 7 measurements). The oxidation process is not reversible (see Fig. S13 for a representative trace); as such, we estimated  $E_{Ox}$  solely from the potential of the anodic peaks. Their optical band gap is between 4.5 and 3.1 eV (Figure 2A). Because the solvent used is polar in nature, the Coulombic term in the above expression ( $e^2/4\pi\epsilon_0\epsilon_r d$ ) can be neglected.

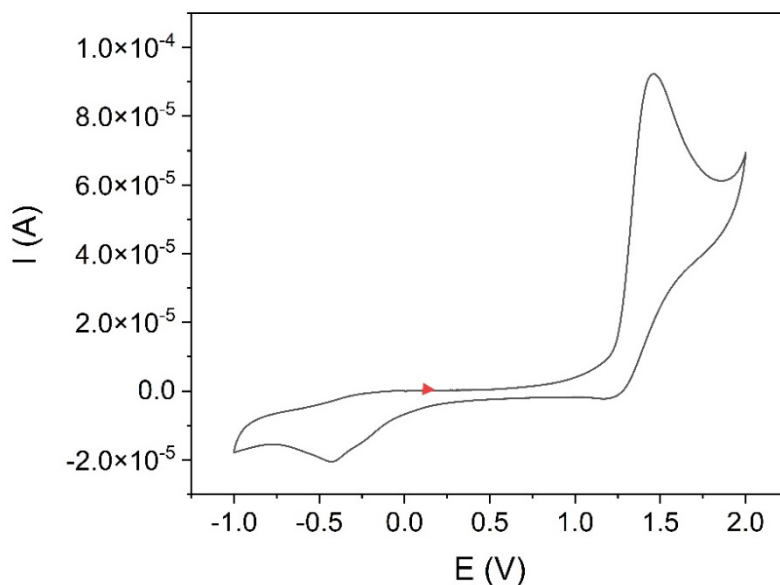


**Figure S13.** Cyclic voltammogram [1 mg/mL, Bu<sub>4</sub>NPF<sub>6</sub> 0.1 M, DMF, 20 °C, 0.1 V s<sup>-1</sup>] of CDs 1.

<sup>3</sup> Kavarnos, G. J. *Fundamentals of Photoinduced Electron Transfer*; VCH: New York, 1993.

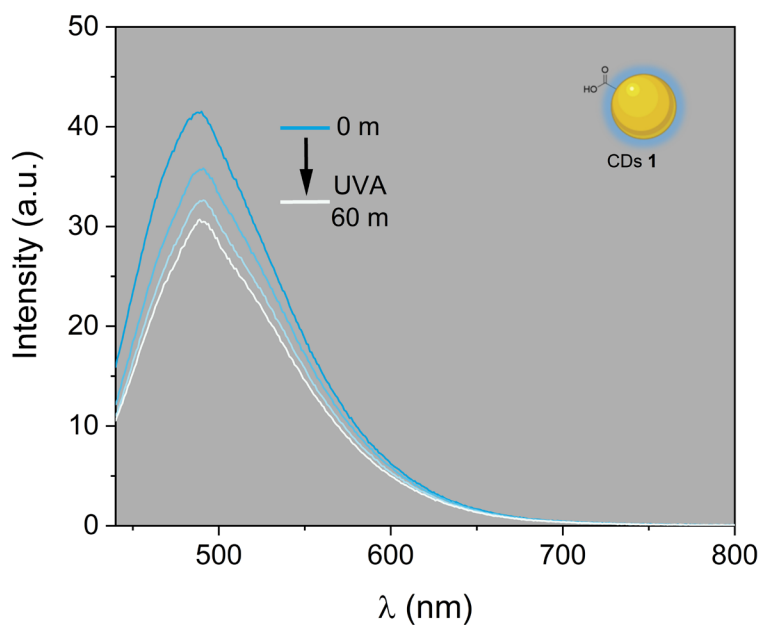


**Figure S14.** Emission spectra (10  $\mu\text{g/mL}$ , 20  $^{\circ}\text{C}$ ,  $\text{H}_2\text{O}$ ,  $\lambda_{\text{Ex}} = 420 \text{ nm}$ ) of CDs **1** before and after ultraviolet irradiation (365 nm, 0-60 min).

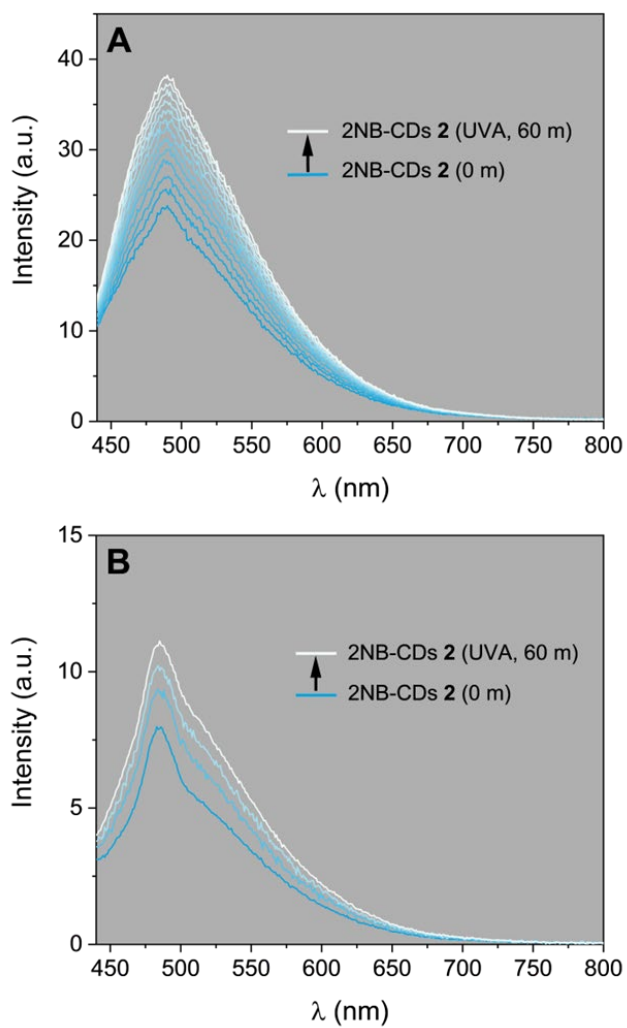


**Figure S15.** Emission spectra (10  $\mu\text{g/mL}$ , 20  $^{\circ}\text{C}$ ,  $\lambda_{\text{EX}} = 420 \text{ nm}$ , blue traces) of 2NB-CDs **2** before and after ultraviolet irradiation in (A)  $\text{H}_2\text{O}$  at pH 3 and (B) 50:50 mixture of  $\text{H}_2\text{O}$  and DMSO.

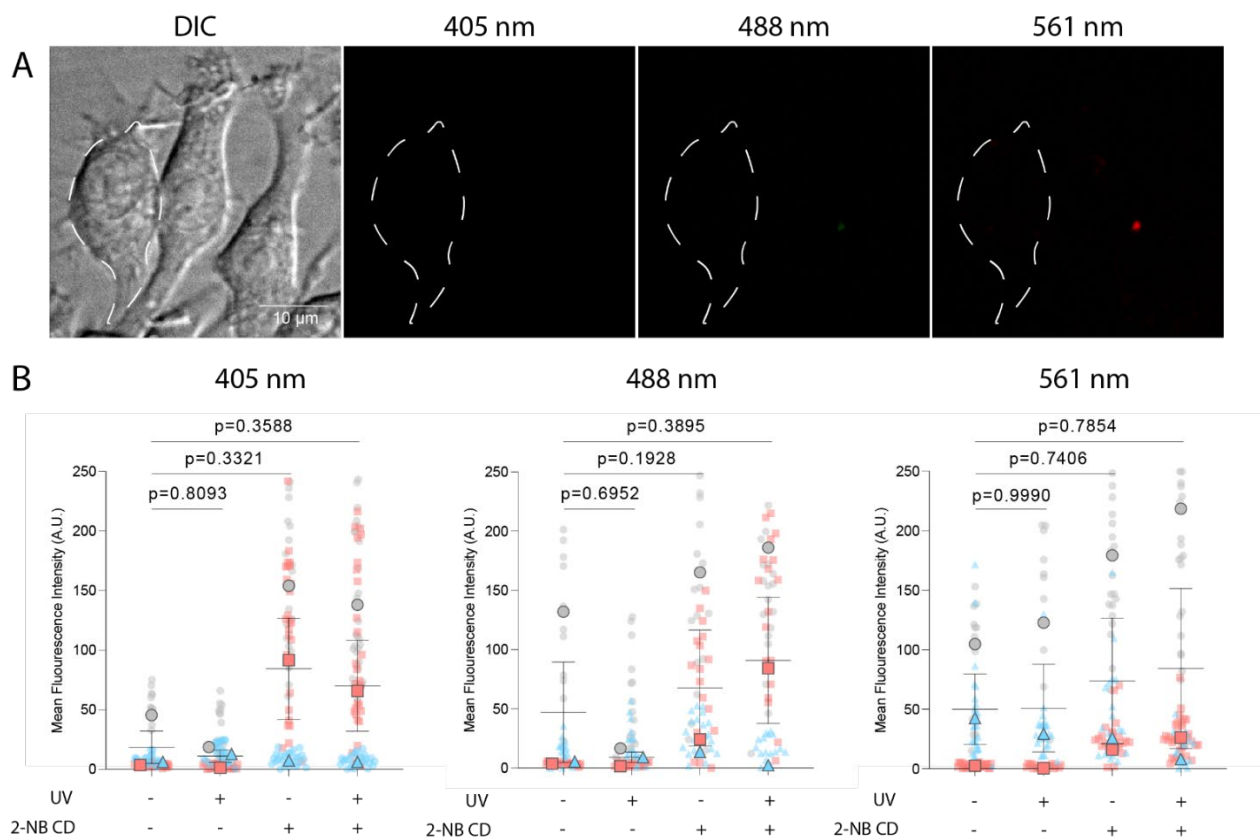


**Figure S16.** (A) Spinning disc confocal microscopy of RAW 264.7 macrophages exposed to 50 mg/ml 2NB-CDs **2** for 30 minutes at different excitation wavelengths. The white dashed outline indicates the position of a cell within the same field of view. (B) Mean fluorescence intensity determined using ImageJ/FIJI. Different colours and shapes indicate replicates,  $n=3$  independent experiments. Outlined symbols indicate mean of replicate, with corresponding smaller symbols representing individual cell value, whereby 30-50 cells were measured per experiment and condition. Data are shown as mean fluorescence intensity per cell  $\pm$  Standard Error of the Mean after background subtraction. Data was analyzed using paired, one-tailed Student's t-test. Significant comparisons used a threshold of  $p < 0.05$ ; actual  $p$  values are shown.